

1 Minor revision after review - 16/12/15

2

3 1) Line 23: "reduce by half". This depends on how many cores are drilled so does not make
4 sense without this information.

5

6 We agree that comment, the text has been modified as follows:

7

8 "

9 [...]can lead to a non-exhaustive record of volcanic events when a single core is used as the
10 site reference with a bulk probability of 30 % of missing volcanic events and close to 65 %
11 uncertainty on one volcanic flux measurement (based on the standard deviation obtained from
12 a 5 cores comparison). Averaging n records reduces significantly (by a factor $1/\sqrt{n}$) the
13 uncertainty of the deposited flux mean; in the case of 5 cores, the uncertainty of the mean flux
14 can therefore be reduced to 29%.

15 This also links to issues around line 300 (later). The point is that the standard deviation
16 around the mean should not change however many cores one drills. But the estimate of the
17 actual volcanic strength is based on the mean and the standard error of the mean reduces as
18 square root of n. Thus the change from 56% to 41% is probably not very meaningful, but if
19 the geometric SD is 41%, then with 5 cores the SE of the mean (ie the uncertainty in the flux)
20 is 18%. Please discuss with a statistician as I may have misunderstood what you did but
21 anyway the statement in line 23 definitely needs a context that it reduces with 5 cores.

22

23

24 We agree that this aspect was unclear in the text, it has been modified as follows. Table 3 has
25 been modified accordingly, and only information of interest were kept. The numbers found
26 differ from the previous version because we decided to calculate the mean of the 5 core fluxes
27 (considering a nil flux in non detected peaks), rather than averaging values in detected peaks
28 (mean = sum of fluxes in detected peaks / number of time the peak is detected among the 5
29 core). We believe this calculation makes more sense, and avoids a bias by taking into account
30 both present and absent peaks.

31

32 "

33 **Variability in signal strength**

34 To compare peak height variability, detected peaks were corrected by subtracting the background from
35 peak maxima. We considered C_i/C_{mean} variations, C_i being the SO_4^{2-} maximum concentration in core i
36 (1 to 5), and C_{mean} being the mean of those concentrations for the event i. C_i is considered nil if the
37 peak is not detected in a core. For concentration values, positive by definition, the log-normal
38 distribution is more appropriate; geometric means and geometric standard deviations were used, as

39 described by *Wolff et al.*, [2005] (Table 3). In our calculation, the geometric standard deviation based
40 on 5 cores is 1.49; in other words, the maximum concentration of a peak in one core is uncertain by
41 49%. This factor is completely in agreement with the one obtained in *Wolff et al.*, [2005] (1.5). Having
42 n cores allows for a reduction of the uncertainty on the mean (standard error of the mean) by a factor
43 $1/\sqrt{n}$. The peak heights mean starting from 5 cores is therefore uncertain by 22%. Comparing peaks
44 maximum induces a bias related to the sampling method: with a two centimeters resolution on average,
45 peak's height is directly impacted by the cutting, which tends to smooth the maxima. Comparing the
46 total sulfate deposited during the event is more appropriate. Proceeding on a similar approach, but
47 reasoning on mass of deposited sulfate rather than maximum concentration (and considering F_i/F_{mean} ,
48 F_i being the mass flux of peak i), the obtained variability is higher than previously. The uncertainty on
49 the flux for one measurement is 65 % (based on the standard deviation of the mean), and the
50 uncertainty of the mean (standard error of the mean) is therefore close to 30%. The difference in the
51 signal dispersion between the two approaches rests on the fact that peak maximum has a tendency to
52 smooth the concentration profile as a consequence of the sampling strategy. This artifact is suppressed
53 when the total mass deposited is considered.

54 "
55

56 2) Around line 156. A good test whether this outlier approach works is to state how many
57 "troughs" are detected if you use an $m-2$ sigma approach. Of course you should have a few
58 individual points that fall below 2 sigma, but if (as i suspect) you don't identify any signals in
59 3 consecutive points, then your outlier detection has worked well.

60
61 This test was performed; no more than two points per core are detected by applying the same
62 test in the negative direction, except in one single case: in core 5, three consecutive points are
63 once detected in the core (data with concentrations around 40ppb). This method clearly
64 discriminates volcanic outliers from natural background fluctuations, as shown by the
65 obtained result.

66
67
68 3) Fig 7. Please expand the caption, I don't think the reader can easily understand what this
69 figure shows. In the 5 core case, 8 sigma (green hatching) I don't think the reader can tell
70 whether 90% is the probability that the peak occurs in a single core, or the probability that it
71 occurs in all 5 cores? i think it's the former, but then is it seen at 8 sigma in all 5 cores? This
72 just needs explaining better what it is.

73
74 The caption was completed as follow in the text:

75 "
76

77 **Figure 7** - Peaks probability to be detected in 2, 3, 4 or 5 cores, as function of their flux. The
78 three categories of flux are defined by peaks flux value, relatively to the average background
79 flux, and quantified by x time (2, 5 and 8) the flux standard deviation (calculated for a 30 ppb
80 standard deviation in concentrations). At flux above *background flux* + 8σ , the volcanic peak
81 has 90% chance to be detected in each core of a population of 5 cores. On the other hand,
82 at flux below background flux + 5σ , the volcanic peak has a probability of 60% to be
83 detected in 2 cores among the 5 cores population. This highlights that replicate cores are
84 particularly useful to avoid missing small to intermediate peaks in a record.

85 "

86 4. Supplement. I appreciate the sentiment to include these figures in response to the reviewer,
87 but other readers will not be able to understand it, unless they read Gfeller. Please add text to
88 explain at least qualitatively what Gfeller's approach is.

89

90 The text was completed as follow (Added line 99):

91 "

92 The representativeness of a volcanic record can be assessed by isolating the volcanic peaks in different
93 records, as done in Wolff's work and in this study, or by a global comparison of the sulfate
94 concentration records as proposed in Gfeller et al. (2014). In the later case, the full individual profiles
95 (background + the volcanic peaks) are compared to a theoretical ideal case made of an infinite
96 number of profiles. A similarity coefficient is then calculated between a population made of n profiles
97 and the infinite population. However, this approach can't be extrapolated to discrete profiles, as in our
98 approach, because there is a priori no ideal profile for the volcanic record. Nevertheless, the
99 representativeness of sulfate in Dome C record, as defined by Gfeller et al. work, has been also
100 calculated for element of comparison with this method, and the result is available in the supplementary
101 online material (fig. S1). "

102

103 The text was also completed in SOM caption:

104

105 "

106 Gfeller *et al.* (2014) method relies on calculating inter-series correlation (expressed as $R_{n,N}$, n
107 being a subset of N time series). To calculate the representativeness of the mean of a given
108 subset of cores, and by letting N going to infinity (simulating a fictive infinite number of
109 cores), Gfeller *et al.* (2014) use the $\hat{R}_{n,\infty}^2$ proxy. We used the same proxy of sulfate
110 representativeness on Dome C 5 cores:

111 "

112

113 5. Also please call out both S figures from the main text, otherwise there is no reason anyone
114 would ever see them.

115

116 Done.

117

118 **Variability of sulfate signal in ice-core records based on five replicate cores**

119

120 Gautier Elsa^{1,2}, Savarino Joël^{1,2}, Erbland Joseph^{1,2}, Lanciki Alyson^{1,2}, Possenti Philippe^{1,2}

121

122 ¹Univ. Grenoble Alpes, LGGE, F-38000 Grenoble, France

123 ²CNRS, LGGE, F-38000 Grenoble, France

124

125 **Abstract**

126 Current volcanic reconstructions based on ice core analysis have significantly improved over

127 the past few decades by incorporating multiple core analysis with high temporal resolution

128 from different parts of the polar regions. Regional patterns of volcanic deposition are based

129 on composite records, built from cores taken at both poles. However, in many cases only a

130 single record at a given site is used for these reconstructions. This assumes that transport and

131 regional meteorological patterns are the only source of the dispersion of the volcanic-products.

132 Here we evaluate the local scale variability of a sulfate profile in a low accumulation site

133 (Dome C, Antarctica), in order to assess the representativeness of one core for such

134 reconstruction. We evaluate the variability with depth, statistical occurrence, and sulfate flux

135 deposition variability of volcanic eruptions detected on 5 ice cores, drilled 1 meter away from

136 each other. Local scale variability, essentially attributed to snow drift and surface roughness

137 at Dome C, can lead to a non-exhaustive record of volcanic events when a single core is used

138 as the site reference with a bulk probability of 30 % of missing volcanic events and close to

139 65 % uncertainty on one volcanic flux measurement (based on the standard deviation obtained

140 from a 5 cores comparison). Averaging n records reduces significantly (by a factor $1/\sqrt{n}$) the

141 uncertainty of the deposited flux mean; in the case of 5 cores, the uncertainty of the mean flux

142 can therefore be reduced to 29%.

143

144 **Introduction**

145 When a large and powerful volcanic eruption occurs, the energy of the blast is sufficient to inject
146 megatons of material directly into the upper atmosphere [Robock, 2000]. While ashes and pyroclastic
147 materials fall rapidly to the ground because of gravity, gases remain over longer time scales. Among
148 gases, SO₂ is of a particular interest due to its conversion to tiny sulfuric acid aerosols, which can
149 potentially impact the radiative budget of the atmosphere [Rampino and Self, 1982; Timmreck, 2012].
150 In the troposphere a combination of turbulence, cloud formation, rainout and downward transport are
151 efficient processes that clean the atmosphere of sulfuric acid, and volcanic sulfuric acid layers rarely
152 survive more than a few weeks, limiting their impact on climate. The story is different when volcanic
153 SO₂ is injected into the stratosphere. There, the dry, cold and stratified atmosphere allows sulfuric acid
154 layers to remain for years, slowly spreading an aerosol blanket around the globe. The tiny aerosols
155 then act as efficient reflectors and absorbers of incoming solar radiations, significantly modifying the
156 energy balance of the atmosphere [Kiehl and Briegleb, 1993] and the ocean [Gleckler et al., 2006;
157 Miller et al., 2012; Ortega et al., 2015]. With a lifetime of 2 to 4 years, these aerosols of sulfuric acid
158 ultimately fall into the troposphere where they are removed within weeks.

159 In Polar Regions, the deposition of the sulfuric acid particles on pristine snow will generate an acidic
160 snow layer, enriched in sulfate. The continuous falling of snow, the absence of melting and the ice
161 thickness make the polar snowpack the best records of the Earth's volcanic eruptions. Hammer [1977]
162 was the first to recognize the polar ice propensity to record such volcanic history. Built on the seminal
163 work of Hammer et al., a paleo-volcanism science developed around this discovery with two aims.

164 The first relies on the idea that the ice record can reveal past volcanic activity and, to a greater extent,
165 its impact on Earth's climate history [Robock, 2000; Timmreck, 2012]. Indeed, at millennium time
166 scale, volcanoes and the solar activity are the two main recognised natural climate forcings [Stocker et
167 al., 2013]. Based on ice records, many attempts are made to extract the climate forcing induced by a
168 volcanic eruption [Crowley and Unterman, 2013 ; Gao et al., 2008; Gao et al., 2007; Sigl et al., 2013;
169 Sigl et al., 2014; Zielinski, 1995]. However, such an approach is inevitably prone to large uncertainty

GAUTIER Elsa 16/12/y 15:06

Supprimé: s

GAUTIER Elsa 16/12/y 15:07

Supprimé: only

GAUTIER Elsa 16/12/y 15:07

Supprimé: z

173 pertaining to the quality of the ice record and non-linear effects between deposition fluxes and source
174 emissions [Pfeiffer *et al.*, 2006].

175 The second aim of the paleo-volcanism is to provide an absolute dating scale when clear volcanic
176 events in differently located ice cores can be unambiguously attributed to the same dated event [Severi
177 *et al.*, 2007]. The time synchronization of different proxy records is possible, allowing study of the
178 phasing response of different environmental parameters to climate perturbation [Ortega *et al.*, 2015;
179 Sigl *et al.*, 2015] or estimating the snow deposition over time [Parrenin *et al.*, 2007]. Whatever the
180 intent, paleo-volcanism should rely on robust and statistically relevant ice core records.

181 Work to establish a volcanic index, undertaken to date, has assumed volcanic events are clearly
182 identified, without any false signal from background variations induced by other sulfur sources (eg
183 marine, anthropogenic, etc.). Seasonal layer counting is used whenever possible, bi-polar comparison
184 of ice sulfate records has become the method of choice to establish an absolute dated volcanic index
185 [Langway *et al.*, 1988]. Both known and unknown events can be used to synchronize different cores.
186 However, only a limited number of peaks, with characteristic shape or intensity, and known to be
187 associated with a dated eruption, can be used to set a reliable time scale [Parrenin *et al.*, 2007]. This
188 restriction is partly fueled by the poor and/or unknown representativeness of most volcanic events
189 found in ice cores. Most of the time, a single core is drilled at a given site and used for cross
190 comparison with other sites. This approach is clearly insufficient for ambiguous events.

191 At a large scale, sulfate deposition is highly variable in space and mainly associated with atmospheric
192 transport and precipitation patterns. At a local scale (ca. 1m), variability can emerge from post-
193 deposition processes. While sulfate is a non-volatile species supposed to be well preserved in snow,
194 spatial variability is induced by drifted snow, wind erosion leading to surface roughness
195 heterogeneities [Libois *et al.*, 2014]. These effects are amplified in low accumulation sites where most
196 of the deep drilling sites are performed [EPICA-community-members, 2004; Jouzel, 2013; Lorius *et al.*,
197 1985]). To the best of our knowledge, one single study has used multiple drillings at a given site to
198 analyze the representativeness of the ice core record [Wolff *et al.*, 2005]. This study took advantage of
199 the two EPICA cores drilled at Dome C, 10 m apart (Antarctica, 75°06'S, 123°21'E, elevation 3220 m,

200 mean annual temperature -54.5°C) [EPICA-community-members, 2004] to compare the dielectric
201 profile (DEP) along the 788 m common length of the two cores. For the two replicate cores, statistical
202 analysis showed that up to 50 % variability in the pattern of any given peak was encountered as a
203 consequence of the spatial variability of the snow deposition. The authors concluded that ice-core
204 volcanic indices from single cores at such low-accumulation sites couldn't be reliable and what was
205 required was a network of close-spaced records. However, as mentioned in Wolff's conclusion, this
206 statistical study relied only on two records. Additionally, DEP signals are known to be less sensitive
207 than sulfate signals for volcanic identification, and more accuracy is expected by comparing sulfate
208 profiles. The authors thus encouraged conducting a similar study on multiple ice cores to see if the
209 uncertainty could be reduced.

210 In the present study we took advantage of the drilling of 5 ice cores at Dome C, initially intended for
211 the analysis of sulfur isotopes of the volcanic sulfate. Putting aside the number of records, our
212 approach is similar in many points to Wolff's work. However, it has the advantage of relying on highly
213 resolved sulfate profiles. In addition, the spatial scale is slightly smaller as the 5 cores were drilled 1-
214 meter apart. The comparison of 5 identically processed cores is a chance to approach the
215 representativeness of a single core reconstruction at a low accumulation site, the most prone to spatial
216 variability. The representativeness of a volcanic record can be assessed by isolating the volcanic peaks
217 in different records, as done in Wolff's work and in this study, or by a global comparison of the sulfate
218 concentration records as proposed in Gfeller et al. (2014). In the later case, the full individual profiles
219 (background + the volcanic peaks) are compared to a theoretical ideal case made of an infinite
220 number of profiles. A similarity coefficient is then calculated between a population made of n profiles
221 and the infinite population. However, this approach can't be extrapolated to discrete profiles, as in our
222 approach, because there is a priori no ideal profile for the volcanic record. Nevertheless, the
223 representativeness of sulfate in Dome C record, as defined by Gfeller et al. work, has been also
224 calculated for element of comparison with this method, and the result is available in the supplementary
225 online material (fig. S1).

226

227 | New constraints on variability of sulfate deposition recorded by spatial heterogeneity in such sites are
228 | expected from the present work. Even if recent publications [Sigl et al., 2014], underline the need of
229 | using multiple records in low accumulation sites, to overcome the spatial variability issue, such
230 | records are not always available. This lack of records adds uncertainty in the volcanic flux
231 | reconstruction based on polar depositional pattern. Our study should help to better constrain the error
232 | associated with local scale variability, and ultimately, the statistical significance of volcanic
233 | reconstructions. The present study discusses the depth shift, occurrence of events and deposition flux
234 | variability observed in the 5 cores drilled.

235

236 | **Experimental setup and Methods**

237 | **Core drilling**

238 | The project “VolSol”, initiated in 2009, aimed at constraining the estimation of the natural part of
239 | radiative forcing, composed of both volcanic and solar contributions using ice core records of sulfate
240 | and ¹⁰Be. In order to build a robust volcanic index including a discrimination of stratospheric events
241 | based on sulfur isotopic ratios [Baroni et al., 2008; Savarino et al., 2003], 5 x 100 m-firn cores (dia.
242 | 10 cm) were drilled in 2010/2011 along a 5 m straight line, and spaced approximately 1 m apart. The
243 | drilling took place at the French-Italian station Concordia, more precisely between Concordia station
244 | and EDC drilling tent (300m west of the EDC drilling tent). At this site, the mean annual snow
245 | accumulation rate is about 25 kg m⁻² y⁻¹, leading to an estimated time-period covered by the cores of
246 | 2500 years. Cores were logged and bagged in the field, and temporarily stored in the underground core
247 | buffer (- 50 °C) before analysis. The unusual number of ice core drilled at the same place was driven
248 | by the amount of sulfate necessary to conduct the isotopic analysis. However, this number of replicate
249 | cores drilled 1m apart offers the opportunity to question the representativeness of a volcanic signal
250 | extracted from a single core per site.

251

252 | **Sampling, Resolution and IC Analyses**

GAUTIER Elsa 16/12/y 11:44

Mis en forme: Police :Non Italique,
Vérifier l'orthographe et la grammaire

GAUTIER Elsa 16/12/y 15:09

Supprimé: Beryllium-

GAUTIER Elsa 16/12/y 15:09

Mis en forme: Exposant

GAUTIER Elsa 16/12/y 15:10

Supprimé: (Dome C, Antarctica, 75°06'S,
123°21'E, elevation 3220 m, mean annual
temperature -54.5°C)

257 | Analyses were directly performed in the field during two consecutive summer campaigns. Thirty
258 | meters were analyzed in 2011, the rest was processed the following year. The protocol was identical
259 | for each core and the steps followed were:

- 260 | - Decontamination of the external layer by scalpel scrapping
- 261 | - Longitudinal cut with a band saw of a 2 cm stick of the most external layer
- 262 | - Sampling of the ice stick at a 2 cm-resolution (ca. 23 600 samples)
- 263 | - Thawing the samples in 50 ml centrifuge tubes, and transfer in 15 ml centrifuge tubes positioned in
264 | an autosampler
- 265 | - Automatic analysis with a Metrohm IC 850 in suppressed mode (NaOH at 7 mM, suppressor H₂SO₄
266 | at 50 mM, Dionex AG11 column), in a fast IC configuration (2 min run) with regular calibration
267 | (every 60 samples) using certified sulfate reference solution (Fisher brand, 1000 ppm certified).

268 | Due to the fragility of snow cores, the first 4 m were only analyzed on a single core (Figure 1). We
269 | will thus not discuss the variability of the Pinatubo and Agung eruptions present in these first 4 meters.
270 | Concentration data are deposited in the public domain and made freely available in NOAA National
271 | Climatic Data center.

272

273 | **Peaks discrimination method**

274 | As with most algorithms used for peak detection, the principle is to detect anomalous sulfate
275 | concentration peaks from a background noise (stationary or not), which could potentially indicate a
276 | volcanic event. The estimation of the background value should therefore be as accurate as possible.
277 | Using core 2 as our reference core, we observed a background average value stationary and close to 85
278 | ppb \pm 30 ppb (1σ) at Dome C during the 2,500 years of the record. However, the variability is
279 | sufficient enough to induce potential confusion on detection of small peaks. Therefore, a stringent
280 | algorithm using PYTHON language (accessible on demand) was developed to isolate each possible
281 | peak. The algorithm treats the full ice record by 1-meter section (ca. 45-50 samples). For each meter, a
282 | mean concentration (m) and standard deviation (σ) is calculated regardless of the presence or not of
283 | peaks in the section. Then, every value above the $m + 2\sigma$ is removed from the 1-meter dataset. A new

285 mean and standard deviation is calculated and the same filtration is applied. Iteration runs until no
286 more data above $m + 2 \sigma$ is found. At that point, m represents the background mean concentration
287 [\(The resulting background estimation along core 1 is illustrated in SOM, figure S2\)](#). The process runs
288 for each 1-m section, starting from the surface sample and until the end of the core. Then, each 1-
289 meter dataset is shifted by one sample; the process is reset and the peak detection run again on each
290 new 1-m dataset. Sample shift is applied until the last sample of the first 1-meter section is reached so
291 that no bias is introduced by the sampling scheme. Every concentration data point is thus compared
292 approximately with its 100 [neighboring](#) data (50 of each side). Each data point isolated by the
293 algorithm is further tested. To be considered as a point belonging to a potential volcanic peak, the data
294 should be detected in a given core (i.e. for being above the $m + 2 \sigma$ final threshold) in at least 50 % of
295 the 50 runs. Additionally, the point has to be part of at least three consecutive points passing the same
296 50 % threshold detection. This algorithm was applied individually on each core, giving 5 different
297 lists of peak. In total, 54, 51, 47, 50 and 47 peaks were detected on core 1, 2, 3, 4 and 5, respectively.
298 A manual detection is then required if one wants to build a more accomplished volcanic record from
299 several profiles, which must be based on shape criteria, and not only statistical criteria. However, in
300 the scope of this paper, no manual sorting was applied, so that the statistical assessment could rely on
301 more objective criteria (the number of occurrences).

302

303 **Core synchronization and dating**

304 Core 1 was entirely dated with respect to the recently published volcanic ice core database [*Sigl et al.*,
305 2015] using *Analyseries* 2.0.8 software (<http://www.lsce.ipsl.fr/Phocea/Page/index.php?id=3>), and
306 covers the time period of -588 to 2010 CE. Figure 2 shows the age-depth profile obtained for this core.
307 A total of 13 major volcanic eruptions well dated were used as time markers to set a time scale (bold
308 date in Table 1). Core 1 was entirely dated through linear interpolation between those tie points. Dated
309 core 1 was then used as a reference to synchronize the remaining 4 cores, using the same tie points and
310 10 additional peaks (non-bold date in Table 1), presenting characteristic patterns common to each core.
311 In total, 23 points were therefore used to synchronize the cores.

312

313 **Composite building from the 5 ice cores**

314 Through the routine described above, the five cores are depth-synchronized using the 23 tie points and
315 other potential volcanic events in each core cores are detected independently. Therefore, the number
316 of peaks detected in each core is different (between 47 and 54) and their depth (with the exception of
317 the tie points used) is slightly different to each other cores due to sampling scheme and position of the
318 maximum concentration. After correcting the depth shift between cores, a composite profile was built
319 by summing all the peaks identified in the 5 cores. In this composite, sulfate peaks from different
320 cores are associated to a same event as soon as their respective depth (corresponding to the maximum
321 concentration) are included in a 20cm depth window. This level of tolerance is consistent with the
322 dispersion in width and shape of peaks observed (Figure 3). A number of occurrences is then
323 attributed to each sulfate peak, reflecting the number of times it has been detected in the 5 cores
324 dataset (Figure 4).

325

326 **Results and Discussions**

327 **Depth offset between cores**

328 Depth offsets between cores are the result of the surface roughness at the time of drilling, variability in
329 snow accumulation, heterogeneous compaction during the burying of snow layers and logging
330 uncertainty. This aspect has been discussed previously, over a similar time-scale (Wolff et al. 2005),
331 and over a longer time-scale (Barnes et al. 2006) in Dome C. Surface roughness, attributed to wind
332 speed, temperatures and accumulation rate, is highly variable in time and space. These small features
333 hardly contribute to the depth offset on a larger spatial scale, in which case glacial flow can control the
334 offset between synchronized peaks, as it seems to be the case in South Pole site (Bay et al. 2010).
335 However, in Dome C, and at the very local spatial scale we are considering in the present work,
336 roughness is significant regarding to the accumulation rate. It is therefore expected that synchronized

GAUTIER Elsa 16/12/y 15:13

Supprimé: p

338 peaks should be found at different depths. The offset trend fluctuates with depth, due to a variable
339 wind speed (Barnes et al. 2006). To estimate the variability in the depth shift for identical volcanic
340 events, we used the tie points listed in Table 1. For each peak maximum, we evaluate the depth offset
341 of core 1, 3, 4 and 5, with respect to core 2. To avoid logging uncertainty due to poor snow
342 compaction in the first meters of the cores and surface roughness at the time of the drilling, we used
343 the UE 1809 depth in core 2 (13.30 m) as a depth reference horizon from which all other depth cores
344 were anchored using the same 1809 event. For this reason, only eruptions prior to 1809 were used to
345 evaluate the offset variability, that is 18 eruptions instead of the 23 used for the core synchronization.
346 Figure 5, shows the distribution of depth shift of the cores with respect to core 2. While the first 40 m
347 appear to be stochastic in nature, a feature consistent with the random local accumulation variations
348 associated with snow drift in Dome C site, it is surprising that at greater depth, offset increases (note
349 that the positive or negative trends are purely arbitrary and depends only on the reference used, here
350 core 2). The maximum offset, obtained between core 3 and 5 is about 40 cm. Such accrued offsets
351 with depth were also observed by *Wolff et al.*, [2005] and were attributed to the process of logging
352 despite the stringent guidelines used during EPICA drilling. Similarly, discontinuities in the depth
353 offset, observed by *Barnes et al.*, [2006] were interpreted as resulting from logging errors. As no
354 physical processes can explain a trend in the offsets, we should also admit that the accrued offset is
355 certainly the result of the logging process. In the field, different operators were involved but a
356 common procedure was used for the logging. Two successive cores extracted from the drill were
357 reassembled on a bench to match the non uniform drill cut and then hand sawed meter by meter to get
358 the best precise depth core, as neither the drill depth recorder nor the length of the drilled core section
359 can be used for establishing the depth scale. This methodology involving different operators should
360 have randomized systematic errors but obviously this was not the case. Despite the systematic depth
361 offset observed, synchronization did not pose fundamental issues as the maximum offset in rescaled
362 profiles never exceeds the peak width (ca. 20 cm) thank to the 10 possible comparisons when pair of
363 core are compared. Confusion of events or missing of events are thus very limited in our analysis (see
364 next section).

365

366 **Variability in events occurrence**

367 The variability in events occurrence in the 5 ice cores has been evaluated through the construction of a
368 composite record (Figure 4) and the counting of events in each core as described in the method. By
369 combining the five ice cores, we listed a total amount of 91 sulfate peaks (Pinatubo and Agung not
370 included), which are not necessarily from volcanic sources. Some peaks can be due to post deposition
371 effects affecting the background deposition, or even contamination. When it comes to defining a
372 robust volcanic index, peak detection issues emerge. Chances to misinterpret a sulfate peak and assign
373 it, by mistake, to a volcanic eruption, as well as chances to miss a volcanic peak, can be discussed
374 through a statistic analysis conducted on our five cores.

375 We try to evaluate to what extent multiple cores comparison facilitates the identification of volcanic
376 peaks, among all sulfate peaks that can be detected in a core. To do so, we assumed that a peak is of
377 volcanic origin as soon as it is detected at least in two cores. In other words, the probability to have
378 two non-volcanic peaks synchronized in two different cores is nil. It is expected that combining an
379 increasing number of cores will increasingly reveal the real pattern of the volcanic events. All possible
380 combinations from 2 to 5 cores comparison were analyzed, totalizing 26 possibilities for the entire
381 population. The results for each comparison were averaged, giving a statistic on the average number of
382 volcanic peaks identified per number of cores compared. The results of the statistical analysis are
383 presented in Figure 6. As expected, in a composite made of 1 to 5 cores, the number of sulfate peaks
384 identified as volcanic peaks (for being detected at least twice) increases with the number of cores
385 combined in the composite. Thus, while only 30 peaks can be identified as volcanic from a two cores
386 study, a study based on 5 cores can yields 62 such peaks. The 5-cores comparison results in the
387 composite profile given in Figure 4a. The initial composite of 93 peaks is reduced to 64 volcanic
388 peaks (Pinatubo and Agung included) after removing the single peaks (Figure 4b). Each characteristic
389 of the retained peaks is given in Table 2. The main conclusion observing the final composite record is
390 that only 17 of the 64 peaks were detected in all of the 5 cores and 68 % of all peaks were at least
391 present in two cores. At the other side of the spectrum, 2-cores analysis reveals that only 33 % (30

392 peaks on average) of the peaks are identified as possible eruptions. Two cores comparison presents
393 still a high risk of not extracting the most robust volcanic profile at low accumulation sites, a
394 conclusion similar to *Wolff et al.*, [2005]. Surprisingly, it can also be noticed that this 5-core
395 comparison doesn't results in an asymptotic ratio of identified volcanic peaks, suggesting that 5 cores
396 are not sufficient either to produce a full picture. High accumulation sites should be prone to less
397 uncertainty; however, this conclusion remains an a priori that still requires a confirmation.

398 Large and small events are not equally concerned by those statistics. Figure 7 shows that the
399 probability of presence is highly dependent on peak flux and the chance to miss a small peak
400 (maximum flux in the window $[f + 2\sigma : f + 5\sigma]$, f being the background average flux) is much higher
401 than the chance to miss a large one (maximum flux above $f + 8\sigma$). However, it is worth noticing that
402 major eruptions can also be missing from the record, as it has already been observed in other studies
403 [*Castellano et al.*, 2005; *Delmas et al.*, 1992]. The most obvious example in our case is the Tambora
404 peak (1815 AD), absent in 2 of our 5 drillings, while presenting an intermediate to strong signal in the
405 others (Figure 8). The reason for the variability in event occurrence has been discussed already by
406 *Castellano et al.*, [2005]. In the present case of close drillings, long-range transport and large-scale
407 meteorological conditions can be disregarded due to the small spatial scale of our study; the snow drift
408 and surface roughness is certainly the main reasons for missing peaks. The fact that two close events
409 as UE 1809 and Tambora are so differently recorded indicates that post-depositional effects can affect
410 the recording of eruptions very variably in time and space.

411

412 **Variability in signal strength**

413 To compare peak height variability, detected peaks were corrected by subtracting the background from
414 peak maxima. We considered C_i/C_{mean} variations, C_i being the SO_4^{2-} maximum concentration in core i
415 (1 to 5), and C_{mean} being the mean of those concentrations for the event i . C_i is considered nil if the
416 peak is not detected in a core. For concentration values, positive by definition, the log-normal
417 distribution is more appropriate; geometric means and geometric standard deviations were used, as
418 described by *Wolff et al.*, [2005] (Table 3). In our calculation, the geometric standard deviation based

GAUTIER Elsa 16/12/y 15:16

Supprimé: how punctual,

GAUTIER Elsa 16/12/y 15:17

Supprimé: post-depositional effects can affect the recording of eruptions.

422 on 5 cores is 1.49; in other words, the maximum concentration of a peak in one core is uncertain by
423 49%. This factor is completely in agreement with the one obtained in *Wolff et al.*, [2005] (1.5). Having
424 n cores allows for a reduction of the uncertainty on the mean (standard error of the mean) by a factor
425 $1/\sqrt{n}$. The peak heights mean obtained from 5 cores is therefore uncertain by 22%. Comparing peaks
426 maximum induces a bias related to the sampling method: with a two centimeters resolution on average,
427 peak's height is directly impacted by the cutting, which tends to smooth the maxima. Comparing the
428 total sulfate deposited during the event is more appropriate. Proceeding on a similar approach, but
429 reasoning on mass of deposited sulfate rather than maximum concentration (and considering F_i/F_{mean} ,
430 F_i being the mass flux of peak i), the obtained variability is higher than previously. The uncertainty on
431 the flux for one measurement is 65 % (based on the standard deviation of the mean), and the
432 uncertainty of the mean (standard error of the mean) is therefore close to 30%. The difference in the
433 signal dispersion between the two approaches rests on the fact that peak maximum has a tendency to
434 smooth the concentration profile as a consequence of the sampling strategy. This artifact is suppressed
435 when the total mass deposited is considered.

436

437 **Conclusion:**

438 This study confirms in many ways previous work on multiple drilling variability [*Wolff et al.*, 2005].
439 As already discussed, peaks flux uncertainty can be significantly reduced (65 % to 29 %) by averaging
440 5 ice-cores signals. A 5-cores composite profile has been built using the criteria that a peak is
441 considered as volcanic if present at least in two cores. We observed that the number of volcanic peaks
442 listed in a composite profile increases with the number of cores considered. With 2 cores, only 33 %
443 of the peaks present in the composite profile are tagged as volcanoes. This percentage increases to
444 68 % with 5 cores. However, we did not observe an asymptotic value, even with 5 cores drilled. A
445 record based on a single record in a low accumulation site is therefore very unlikely to be a robust
446 volcanic record. Of course, peaks presenting the largest flux are more likely to be detected in any
447 drilling, but the example of the Tambora shows that surface topography is variable enough to erase
448 even the most significant signal, although rarely. This variability in snow surface is evidenced in the

GAUTIER Elsa 16/12/y 16:07

Supprimé: .5

450 depth offset between two cores drilled less than 5 meters from each other, as peaks can easily be
451 situated 40 cm apart.

452 In low accumulation sites such as Dome C, where surface roughness can be on the order of the snow
453 accumulation and highly variable, indices based on chemical records should be considered with
454 respect to the time-scale of the proxy studied. Large time-scale trends are faintly sensitive to this effect.
455 On the contrary, a study on episodic events like volcanic eruptions or biomass burning, with a
456 deposition time in the order of magnitude of the surface variability scale should be based on a
457 multiple-drilling analysis. A network of several cores is needed to obtain a representative record, at
458 least in terms of recorded events. However, although lowered by the number of cores, the flux remains
459 highly variable, and [the mean flux obtained from 5 cores is](#) still uncertain [almost 30%](#). This point is
460 particularly critical in volcanic reconstructions that rely on the deposited flux to estimate the mass of
461 aerosols loaded in the stratosphere, and to a larger extent, the climatic forcing induced. Recent
462 reconstructions largely take into account flux variability associated with regional pattern of deposition,
463 but this study underlines the necessity of not neglecting local scale variability in low accumulation
464 sites. Less variability is expected with higher accumulation rate, but this still has to be demonstrated.
465 Sulfate flux is clearly one of the indicators of the eruption strength, but due to transport, deposition
466 and post-deposition effects, such direct link should not be taken for granted.

467 With such statistical analysis performed systematically at other sites, we should be able to reveal even
468 the smallest imprinted volcanoes in ice cores, extending the absolute ice core dating, the
469 teleconnection between climate and volcanic events and improving the time-resolution of mass
470 balance calculation of ice sheets.

471

472

473 **Acknowledgments**

474 Part of this work would not have been possible without the technical support from the C2FN (French
475 National Center for Coring and Drilling, handled by INSU. Financial supports were provided by
476 LEFE-IMAGO, a scientific program of the Institut National des Sciences de l'Univers (INSU/CNRS),
477 the Agence Nationale de la Recherche (ANR) via contract NT09-431976- VOLSOL and by a grant
478 from Labex OSUG@2020 (Investissements d'avenir – ANR10 LABX56). E. G. deeply thanks the
479 Fulbright commission for providing the PhD Fulbright fellowship. The Institute Polaire Paul-Emile
480 Victor (IPEV) supported the research and polar logistics through the program SUNITEDC No. 1011.
481 We would also like to thank all the field team members present during the VOLSOL campaign and
482 who help us. Data are available at the World Data Center for paleoclimatology
483 (<http://www.ncdc.noaa.gov/paleo/wdc-paleo.html>).

484

485

486

487

488 **References**

489

490 Baroni, M., J. Savarino, J. Cole-Dai, V. K. Rai, and M. H. Thiemens (2008), Anomalous sulfur isotope
491 compositions of volcanic sulfate over the last millennium in Antarctic ice cores, *J Geophys Res*,
492 *113*(D20), D20112, doi: 10.1029/2008jd010185.

493 Barnes, P. R. F., E. W. Wolff, and R. Mulvaney (2006), A 44 kyr paleoroughness record of the
494 Antarctic surface, *J. Geophys. Res.*, 111, D03102, doi:10.1029/2005JD006349.

495 Bay, R. C., R. A. Rohde, P. B. Price, and N. E. Bramall (2010), South Pole paleowind from automated
496 synthesis of ice core records, *J. Geophys. Res.-Atmos.*, 115, doi:10.1029/2009jd013741.

497 Castellano, E., S. Becagli, M. Hansson, M. Hutterli, J. R. Petit, M. R. Rampino, M. Severi, J. P.
498 Steffensen, R. Traversi, and R. Udisti (2005), Holocene volcanic history as recorded in the sulfate

499 stratigraphy of the European Project for Ice Coring in Antarctica Dome C (EDC96) ice core, *J*
500 *Geophys Res*, *110*(D6), D06114, doi: 10.1029/2004jd005259.

501 Crowley, T. J., and M. B. Unterman (2013), Technical details concerning development of a 1200 yr
502 proxy index for global volcanism, *Earth Syst. Sci. Data*, *5*(1), 187-197, doi: 10.5194/essd-5-187-2013.

503 Delmas, R. J., S. Kirchner, J. M. Palais, and J. R. Petit (1992), 1000 years of explosive volcanism
504 recorded at the South-Pole, *Tellus Ser. B-Chem. Phys. Meteorol.*, *44*(4), 335-350.

505 EPICA-community-members (2004), Eight glacial cycles from an Antarctic ice core, *Nature*, *429*,
506 623-628, doi: 10.1038/nature02599.

507 Gao, C., A. Robock, and C. Ammann (2008), Volcanic forcing of climate over the past 1500 years: An
508 improved ice core-based index for climate models, *J Geophys Res*, *113*(D23), D23111, doi:
509 10.1029/2008jd010239.

510 Gao, C., L. Oman, A. Robock, and G. L. Stenchikov (2007), Atmospheric volcanic loading derived
511 from bipolar ice cores: Accounting for the spatial distribution of volcanic deposition, *J Geophys Res*,
512 *112*(D9), D09109, doi: 10.1029/2006jd007461.

513 Gleckler, P. J., K. AchutaRao, J. M. Gregory, B. D. Santer, K. E. Taylor, and T. M. L. Wigley (2006),
514 Krakatoa lives: The effect of volcanic eruptions on ocean heat content and thermal expansion,
515 *Geophys Res Lett*, *33*(17), L17702, doi: 10.1029/2006gl026771.

516 Hammer, C. U. (1977), Past Volcanism Revealed by Greenland Ice Sheet Impurities, *Nature*,
517 *270*(5637), 482-486.

518 Jouzel, J. (2013), A brief history of ice core science over the last 50 yr, *Climate of the Past*, *9*(6),
519 2525-2547, doi: 10.5194/cp-9-2525-2013.

520 Kiehl, J. T., and B. P. Briegleb (1993), The Relative Roles of Sulfate Aerosols and Greenhouse Gases
521 in Climate Forcing, *Science*, *260*(5106), 311-314, doi: 10.1126/science.260.5106.311.

522 Langway, C. C., H. B. Clausen, and C. U. Hammer (1988), An inter-hemispheric volcanic time-
523 marker in ice cores from Greenland and Antarctica, *Annals of Glaciology*, *10*, 102-108.

524 Libois, Q., G. Picard, L. Arnaud, S. Morin, and E. Brun (2014), Modeling the impact of snow drift on
525 the decameter-scale variability of snow properties on the Antarctic Plateau, *Journal of Geophysical*

526 *Research: Atmospheres*, 119(20), 11,662-611,681, doi: 10.1002/2014jd022361.

527 Lorius, C., J. Jouzel, C. Ritz, L. Merlivat, N. I. Barkov, Y. S. Korotkevich, and V. M. Kotlyakov
528 (1985), A 150,000-year climatic record from Antarctic ice, *Nature*, 316(6029), 591-596, doi:
529 10.1038/316591a0.

530 Miller, G. H., Geirsdóttir, Á., Zhong, Y., Larsen, D. J., Otto-Bliesner, B. L., Holland, M. M., Bailey,
531 D. a., Refsnider, K. a., Lehman, S. J., Southon, J. R., Anderson, C., Björnsson, H. and Thordarson, T.
532 (2012), Abrupt onset of the Little Ice Age triggered by volcanism and sustained by sea-ice/ocean
533 feedbacks, *Geophys. Res. Lett.*, 39(2), L02708, doi: 10.1029/2011gl050168.

534 Ortega, P., F. Lehner, D. Swingedouw, V. Masson-Delmotte, C. C. Raible, M. Casado, and P. Yiou
535 (2015), A model-tested North Atlantic Oscillation reconstruction for the past millennium, *Nature*,
536 523(7558), 71-74, doi: 10.1038/nature14518.

537 Parrenin, F., Barnola, J.-M., Beer, J., Blunier, T., Castellano, E., Chappellaz, J., Dreyfus, G., Fischer,
538 H., Fujita, S., Jouzel, J., Kawamura, K., Lemieux-Dudon, B., Loulergue, L., Masson-Delmotte, V.,
539 Narcisi, B., Petit, J.-R., Raisbeck, G., Raynaud, D., Ruth, U., Schwander, J., Severi, M., Spahni, R.,
540 Steffensen, J. P., Svensson, a., Udisti, R., Waelbroeck, C. and Wolff, E. W. (2007), The EDC3
541 chronology for the EPICA dome C ice core, *Climate of the Past*, 3(3), 485-497, doi: 10.5194/cp-3-
542 485-2007.

543 Pfeiffer, M. A., B. Langmann, and H. F. Graf (2006), Atmospheric transport and deposition of
544 Indonesian volcanic emissions, *Atmos Chem Phys*, 6, 2525-2537, doi:10.5194/acp-6-2525-2006.

545 Rampino, M. R., and S. Self (1982), Historic eruptions of Tambora (1815), Krakatau (1883), and
546 Agung (1963), their stratospheric aerosols, and climatic impact, *Quat. Res.*, 18(2), 127-143, doi:
547 10.1016/0033-5894(82)90065-5.

548 Robock, A. (2000), Volcanic eruptions and climate, *Reviews of Geophysics*, 38(2), 191-219.

549 Savarino, J., A. Romero, J. Cole-Dai, S. Bekki, and M. H. Thiemens (2003), UV induced mass-
550 independent sulfur isotope fractionation in stratospheric volcanic sulfate, *Geophys Res Lett*, 30(21),
551 2131, doi: 10.1029/2003gl018134.

552 Severi, M., Becagli, S., Castellano, E., Morganti, a., Traversi, R., Udisti, R., Ruth, U., Fischer, H.,

553 Huybrechts, P., Wolff, E. W., Parrenin, F., Kaufmann, P., Lambert, F. and Steffensen, J. P. (2007),
554 Synchronisation of the EDML and EDC ice cores for the last 52 kyr by volcanic signature matching,
555 *Clim. Past*, 3(3), 367-374, doi: 10.5194/cp-3-367-2007.

556 Sigl, M., McConnell, J. R., Layman, L., Maselli, O., Megwire, K., Pasteris, D., Dahl-jensen, D.,
557 Steffensen, J. P., Vinther, B., Edwards, R., Mulvaney, R. and Kipfstuhl, S. (2013), A new bipolar ice
558 core record of volcanism from WAIS Divide and NEEM and implications for climate forcing of the
559 last 2000 years, *Journal of Geophysical Research: Atmospheres*, 118(3), 1151-1169, doi:
560 10.1029/2012jd018603.

561 Sigl, M., McConnell, J. R., Toohey, M., Curran, M., Das, S. B., Edwards, R., Isaksson, E., Kawamura,
562 K., Kipfstuhl, S., Krüger, K., Layman, L., Maselli, O. J., Motizuki, Y., Motoyama, H. and Pasteris, D.
563 R. (2014), Insights from Antarctica on volcanic forcing during the Common Era, *Nature Clim. Change*,
564 4(8), 693-697, doi: 10.1038/nclimate2293.

565 Sigl, M., Winstrup, M., McConnell, J. R., Welten, K. C., Plunkett, G., Ludlow, F., Büntgen, U., Caffee,
566 M., Chellman, N., Dahl-Jensen, D., Fischer, H., Kipfstuhl, S., Kostick, C., Maselli, O. J., Mekhaldi, F.,
567 Mulvaney, R., Muscheler, R., Pasteris, D. R., Pilcher, J. R., Salzer, M., Schüpbach, S., Steffensen, J.
568 P., Vinther, B. M. and Woodruff, T. E. (2015), Timing and climate forcing of volcanic eruptions for
569 the past 2,500 years, *Nature*, doi: 10.1038/nature14565.

570 Stocker, T. F., Qin, G.-K., Plattner, M., Tignor, S. K., Allen, J., Boschung, A., Nauels, Y., Xia, B. V.,
571 and M. P. M. (2013), IPCC, 2013: The Physical Science Basis, Fifth Assessment Report of the
572 Intergovernmental Panel on Climate Change, Intergovernmental Panel on Climate Change 2013,
573 United Kingdom and New York, NY, USA.

574 Timmreck, C. (2012), Modeling the climatic effects of large explosive volcanic eruptions, *Wiley*
575 *Interdiscip. Rev.-Clim. Chang.*, 3(6), 545-564, doi: 10.1002/wcc.192.

576 Wolff, E. W., E. Cook, P. R. F. Barnes, and R. Mulvaney (2005), Signal variability in replicate ice
577 cores, *Journal of Glaciology*, 51(174), 462-468, doi: 10.3189/172756505781829197.

578 Zielinski, G. A. (1995), Stratospheric loading and optical depth estimates of explosive volcanism over
579 the last 2100 years derived from the Greenland- Ice-Sheet-Project-2 ice core, *J Geophys Res*,

580 100(D10), 20937-20955.

581

582 **Table 1** – Tie points used to set the time scale and synchronize the cores. Volcanic events are

583 named "Ev x" if they are not assigned to a well-known eruption. Dating of the events is based

584 on *Sigl et al.*, [2015].

585

Eruption	core 1	core 2	core 3	core 4	core 5	date of deposition
Surface	0	0	0	0	0	2010
Pinatubo	1.53					1992
Krakatoa	8.82	8.92	8.67	8.71	8.63	1884
Cosiguina	11.98	11.83	11.65	11.62	11.46	1835
Tambora	12.85			12.6	12.57	1816
UE 1809	13.33	13.3	13.04	13.08	12.98	1809
ev 7	15.98	15.93	15.66	15.67	15.52	1762
Serua/UE	19.29	19.22	18.93	18.94	18.78	1695
Ev 10	21.87	21.74	21.53	21.48	21.4	1646
kuwae	30.18	30.04	29.92	29.85	29.73	1459
ev 16 - A	37.35	37.29	37.17	37.04	36.91	1286
ev 16 - B	37.77	37.77	37.62	37.52	37.4	1276
ev 16 - C	38.1	38.04		37.78		1271
Samalas	38.49	38.46	38.28	38.2	38.09	1259
ev 17	39.59	39.56	39.46	39.36	39.2	1230
ev 18	41.87	41.83	41.7	41.6	41.41	1172
ev 22	50.26	50.3	50.2	50.11	49.87	9599
ev 27	60.77	60.72	60.66		60.27	684
ev 31	65.72	65.74	65.68	65.6	65.25	541
ev 35	76.06	76.13	76	75.94	75.64	235
ev 46	90.42	90.53	90.36	90.41	89.95	-214
ev 49	97.15	97.16	97.19	97.22	96.74	-426
ev 51	100.16	100.19		100.22	99.7	-529

586

587

588 **Table 2** – Sulfate peak (maximum concentration, in ng.g^{-1} , and flux of volcanic sulfate
589 deposited, in kg.km^{-2}) considered as volcanic eruptions based on the statistical analysis of the
590 5 cores. Flux is calculated by integrating the peak, using the density profile obtained during
591 the logging process. Volcanic flux values are corrected from background sulfate (calculated
592 separately for each sulfate peak). 0 stands for non-detected events in the cores. Agung
593 (3.77m) and Pinatubo (1.52m) were not included in the statistical analysis because they were
594 analyzed only in core one and thus are marked as not applicable (N/A). The estimation of the
595 average volcanic flux takes into account undetected peaks, for which the flux is considered 0.
596 The relative error on the flux (estimated as 10%) takes into account the IC measurement
597 relative standard deviation (below 4% based on standards runs), the error on firm density
598 (relative error estimated as 2%) and the error on samples time length (10%). The last column
599 displays data obtained from Castellano *et al.* (2005), for identical volcanic peaks. For similar
600 peaks Castellano's flux generally falls into the average flux + 40% uncertainty, sometimes
601 exceeding this value.

Peak depth (m)	date (year)	core 1		core 2		core 3		core 4		core 5		average*		
		[SO ₄ ²⁻] (ng.g ⁻¹)	Volcanic flux (kg / km ²)	[SO ₄ ²⁻] (ng.g ⁻¹)	Volcanic flux (kg / km ²)	[SO ₄ ²⁻] (ng.g ⁻¹)	Volcanic flux (kg / km ²)	[SO ₄ ²⁻] (ng.g ⁻¹)	Volcanic flux (kg / km ²)	[SO ₄ ²⁻] (ng.g ⁻¹)	Volcanic flux (kg / km ²)	[SO ₄ ²⁻] (ng.g ⁻¹)	Volcanic flux (kg / km ²)	1σ (flux)
1.52	1992	188	5.0	N/A	N/A	N/A	N/A	N/A	N/A	N/A	N/A	188	5.0	0.5
3.77	1964	207	5	N/A	N/A	N/A	N/A	N/A	N/A	N/A	N/A	N/A	N/A	N/A
6.24	1929	0	0.0	164	1.3	0	0.0	132	1.1	0	0.0	148	0.5	0.0
8.59	1891	0	0.0	0	0.0	0	0.0	134	1.3	117	0.9	126	0.4	0.0
8.92	1885	232	8.1	262	8.8	236	10.5	240	10.2	216	7.7	237	9.1	0.9
11.83	1839	220	7.7	173	5.4	190	4.9	177	5.5	173	4.0	187	5.5	0.6
12.08	1834	0	0.0	0	0.0	144	2.5	0	0.0	137	1.3	140	0.8	0.1
12.91	1816	455	13.1	0	0.0	0	0.0	188	1.8	307	6.0	317	4.2	0.4
13.3	1809	436	16.6	291	10.5	392	12.7	408	16.3	461	13.4	398	13.9	1.4
15.93	1762	176	2.7	248	6.7	201	3.4	0	0.0	0	0.0	208	2.5	0.3
19.29	1695	287	13.4	0	0.0	168	9.2	194	7.3	0	0.0	217	6.0	0.6
20.3	1674	261	7.8	0	0.0	0	0.0	196	4.3	178	2.3	212	2.9	0.3
20.7	1666	0	0.0	0	0.0	0	0.0	123	1.6	149	2.4	136	0.8	0.1
21.74	1646	257	10.1	249	10.3	259	13.2	282	17.5	257	13.2	261	12.8	1.3
22.72	1625	181	4.8	146	2.7	141	2.9	0	0.0	0	0.0	156	2.1	0.2
23.77	1600	225	10.6	0	0.0	170	2.5	0	0.0	0	0.0	197	2.6	0.3
25.78	1557	144	2.1	0	0.0	0	0.0	148	2.2	0	0.0	146	0.9	0.1
30	1459	496	33.2	442	31.1	422	31.6	543	37.2	559	36.9	493	34.0	3.4
30.56	1449	0	0.0	143	1.8	131	2.8	0	0.0	0	0.0	137	0.9	0.1
31.83	1417	0	0.0	0	0.0	0	0.0	155	2.6	148	2.6	151	1.0	0.1
33.51	1377	0	0.0	0	0.0	140	2.3	0	0.0	162	5.4	151	1.5	0.2
34.85	1348	273	12.4	288	14.2	209	7.9	303	18.3	269	13.2	268	13.2	1.3
37.29	1286	325	18.3	324	16.1	373	17.1	347	14.8	458	30.7	365	19.4	1.9
37.77	1276	563	28.9	605	40.4	570	28.8	525	26.3	497	21.6	552	29.2	2.9
38.04	1271	205	4.1	180	3.1	0	0.0	235	5.1	0	0.0	206	2.5	0.2

38.46	1259	1086	59.7	1022	63.8	928	61.4	1030	78.5	1428	104.8	1099	73.6	7.4
39.25	1239	0	0.0	0	0.0	132	2.6	147	2.4	151	2.7	143	1.5	1.5
39.56	1230	268	17.8	260	16.8	279	15.6	315	18.7	320	16.7	288	17.1	1.7
41.17	1191	0	0.0	216	4.2	247	12.9	0	0.0	241	7.3	235	4.9	0.5
41.83	1172	437	30.9	401	29.4	377	25.2	378	23.3	433	29.4	405	27.6	2.8
44.4	1111	186	5.3	0	0.0	243	5.4	225	9.7	195	6.2	212	5.3	0.5
44.87	1099	174	2.5	0	0.0	0	0.0	153	2.4	0	0.0	163	1.0	0.1
45.81	1075	129	1.6	144	2.3	0	0.0	0	0.0	0	0.0	137	0.8	0.1
47.15	1041	187	3.6	193	3.6	217	4.4	0	0.0	203	6.2	200	3.6	0.4
47.5	1031	192	7.0	163	5.0	166	3.1	0	0.0	198	4.5	180	3.9	0.4
48	1018	0	0.0	155	3.2	168	2.8	0	0.0	0	0.0	161	1.2	0.1
49.63	976	132	2.0	0	0.0	139	2.5	0	0.0	0	0.0	135	0.9	0.1
50.3	959	209	8.2	256	15.6	236	12.6	220	11.9	227	12.1	230	12.1	1.2
52.49	902	254	3.9	0	0.0	215	4.8	184	5.9	233	7.7	222	4.5	0.4
54.35	852	0	0.0	0	0.0	0	0.0	155	2.3	249	5.2	202	1.5	0.1
55.65	819	184	8.8	193	7.3	191	6.7	181	7.1	249	5.2	200	7.0	0.7
58.26	749	155	3.2	202	3.4	0	0.0	201	6.6	0	0.0	186	2.6	0.3
60.72	684	287	12.9	216	14.0	243	7.8	0	0.0	230	4.9	244	7.9	0.8
64.49	577	528	36.0	0	0.0	430	25.8	367	21.4	393	23.3	430	21.3	2.1
65.74	541	287	19.1	274	12.7	283	20.5	306	21.5	304	16.3	291	18.0	1.8
68.41	465	132	2.9	0	0.0	182	4.4	0	0.0	0	0.0	157	1.5	0.1
69.41	436	194	10.7	168	3.8	0	0.0	207	11.1	233	9.1	201	7.0	0.7
72.38	352	0	0.0	172	4.7	203	5.3	0	0.0	188	5.8	188	3.2	0.3
73.13	331	0	0.0	169	4.1	152	2.8	0	0.0	0	0.0	160	1.4	0.1
73.95	304	0	0.0	0	0.0	171	3.7	190	5.7	0	0.0	180	1.9	0.2
76.13	235	205	12.1	258	20.0	237	21.7	287	23.8	262	13.0	250	18.1	1.8
77.17	206	179	5.4	206	15.4	211	12.5	219	13.2	272	13.5	217	12.0	1.2
78.31	172	250	15.3	0	0.0	156	4.3	203	5.4	219	7.7	207	6.6	0.7
79.98	125	165	4.4	187	3.7	0	0.0	162	3.2	167	3.3	170	2.9	0.3
84.5	-4	202	9.8	199	7.7	222	5.0	0	0.0	188	7.9	203	6.1	0.6
85.44	-37	0	0.0	155	4.4	0	0.0	0	0.0	240	8.6	197	2.6	0.3
87.89	-128	236	11.2	212	9.6	270	12.9	244	12.1	0	0.0	241	9.1	0.9
89.28	-173	0	0.0	0	0.0	0	0.0	190	5.6	164	3.7	177	1.9	0.2
90.53	-214	276	18.8	286	26.1	278	16.5	296	18.1	241	6.9	275	17.3	1.7
91.72	-251	0	0.0	0	0.0	0	0.0	227	10.4	244	12.5	236	4.6	0.5
94.83	-347	0	0.0	191	4.6	198	5.9	216	8.7	0	0.0	201	3.8	0.4
97.16	-426	331	22.6	228	15.4	403	35.2	436	48.5	675	75.0	414	39.3	3.9
97.31	-431	0	0.0	131	2.9	0	0.0	0	0.0	0	0.0	65	0.6	0.1
100.19	-529	219	12.1	224	6.6	0	0.0	247	15.9	235	7.7	231	8.5	0.8

602

603

604

605

606

607

608

609

610 **Table 3** – Statistics on sulfate signal for identical peaks in core 1, 2, 3, 4 and 5. Geometric
 611 standard deviations are calculated on peaks heights (i.e maximum concentration reached, in
 612 ng.g⁻¹) and on peaks sulfate flux (i.e total mass of volcanic sulfate deposited after the
 613 eruption). Background corrections are based on background values calculated separately for
 614 each volcanic event.

Study	Number of compared cores	Geom. std deviation based on maximum concentration	Geom std deviation based on deposition flux
Wolff and others	2	1.5	
<u>This study</u>	<u>5</u>	<u>1.49</u>	<u>1.65</u>

615
 616
 617
 618
 619
 620
 621
 622
 623
 624
 625
 626
 627
 628

629
630
631
632
633
634
635
636
637
638
639
640
641
642
643
644
645
646

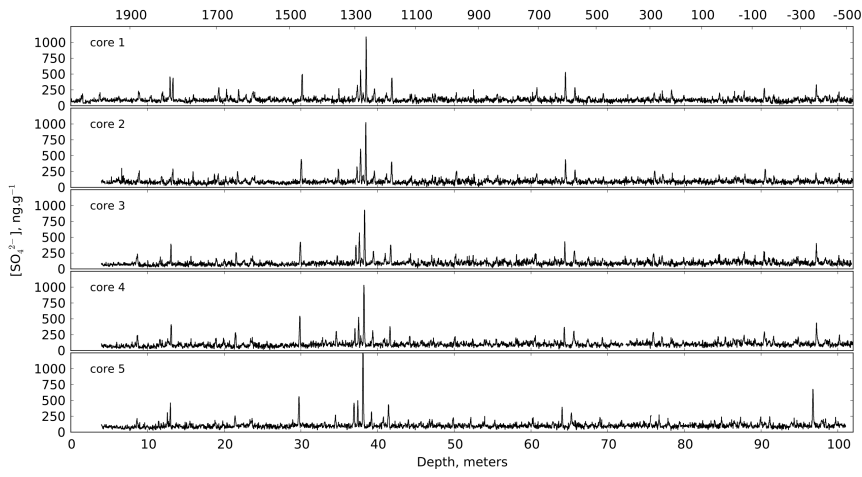
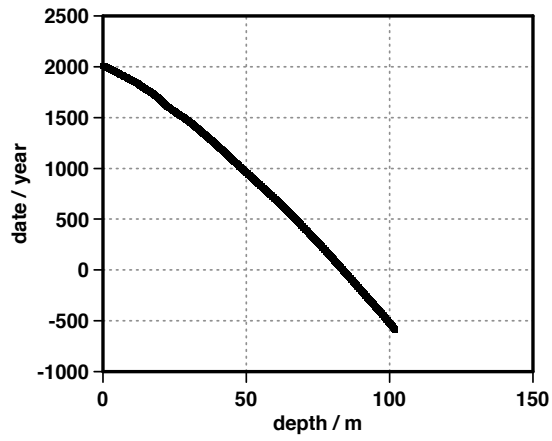
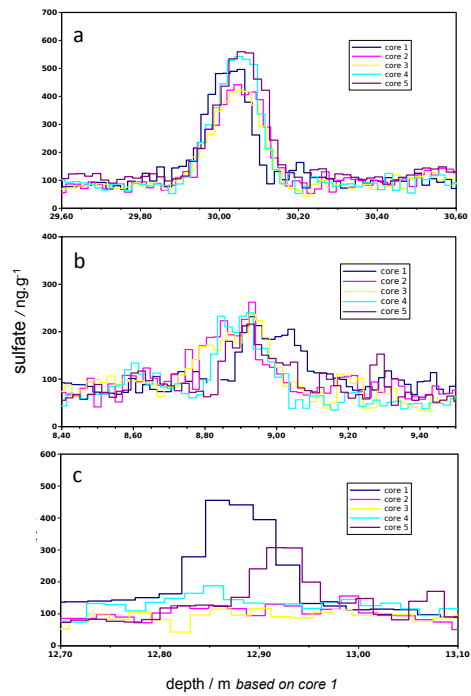


Figure 1 - Sulfate profiles on the 5 replicate cores obtained during a drilling operation at Dome C – Antarctica in 2011.



647
648
649
650
651

Figure 2 - Age versus depth in core 1 drilled in 2011 CE, Dome C – Antarctica



653

654 **Figure 3** –Kuwae (a, top), Krakatoa (b, middle) and Tambora (c, bottom) sulfate

655 concentration profiles after depth synchronization. All peaks are within a 20 cm uncertainty,

656 enabling to clearly attribute each occurrence to a single event.

657

658

659

660

661

662

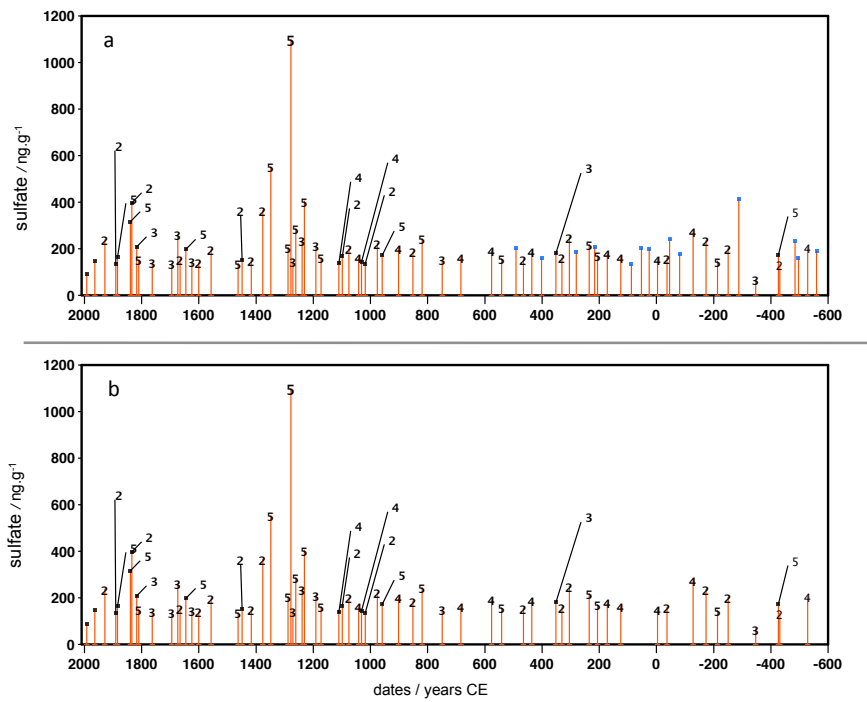
663

664

665

666

667

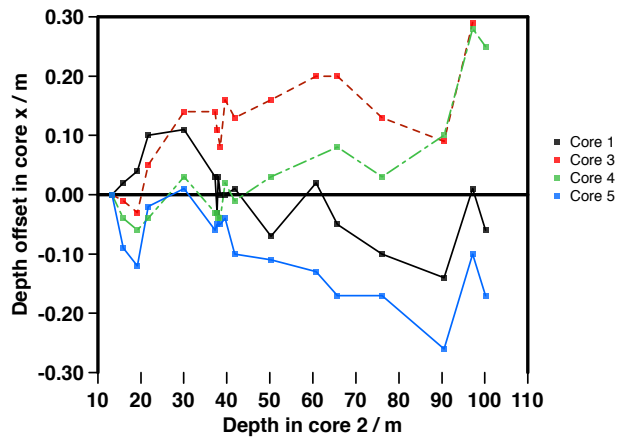


668

669 **Figure 4** – a) Composite sulfate peak profile deduced from our statistical analysis of the 5
670 cores using our detection peak and synchronization algorithms (see text). The numbers
671 indicate the number of time a common peak is found in the cores. Unnumbered peaks, peaks
672 found only in single core. b) same as a) without the single detected peaks. All the remaining
673 peaks are considered as volcanic eruptions. See Table 2 for details.

674

675



676

677

678 **Figure 5** – Depth offset of 18 common and well-identified volcanic events in cores 1, 3, 4 and

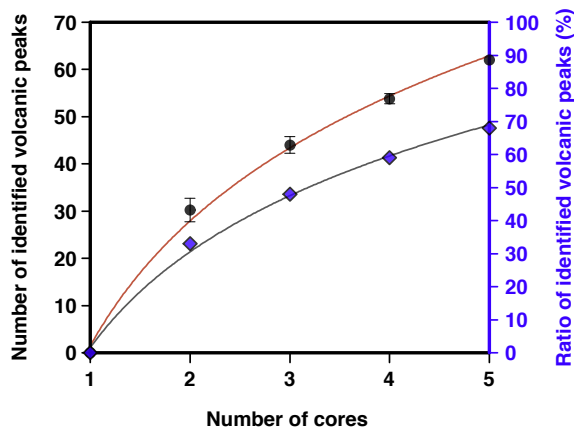
679 5 relatively to core 2. To overcome offset due to the drilling process and poor core quality on

680 the first meters, UE 1809 (depth ca. 13 m) is taken as the origin and horizon reference.

681

682

683



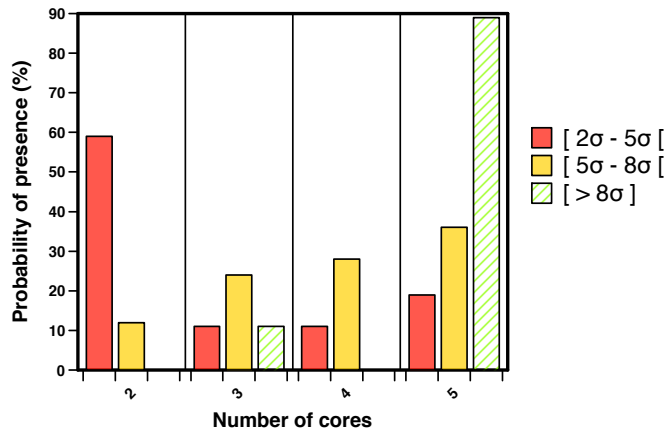
684

685

686 **Figure 6** – Black dots with red line (left axis) represent the number of sulfate peaks that can
687 be identified as volcanic peaks in a composite profile, made of n cores (with n ranging from 1
688 to 5). A sulfate peak appearing simultaneously in at least two cores is considered to be a
689 volcanic peak. Blue diamonds represent the ratio of identified volcanic peaks, i.e the number
690 of identified volcanic peaks (plotted on the left axis), relatively to the total number of sulfate
691 peaks (no discrimination criteria) in a composite made of 5 cores. In our case, the 5 ice-cores
692 composite comprises 91 sulfate peaks (Agung and Pinatubo excluded). With two cores, only
693 33% of them would be identified as being volcanic peaks (detected in both cores), while 68%
694 of them can be identified as volcanic events using 5 cores.

695

696
697
698



699

700 **Figure 7** - Peaks probability to be detected in 2, 3, 4 or 5 cores, as function of their flux. The
701 three categories of flux are defined by peaks flux value, relatively to the average background
702 flux, and quantified by x time (2, 5 and 8) the flux standard deviation (calculated for a 30 ppb
703 standard deviation in concentrations). At flux above $background\ flux + 8\sigma$, the volcanic peak
704 has 90% chance to be detected in each core of a population of 5 cores. On the other hand,
705 at flux below $background\ flux + 5\sigma$, the volcanic peak has a probability of 60% to be
706 detected in 2 cores only, among the 5 cores population. This highlights that replicate cores are
707 particularly useful to avoid missing small to intermediate peaks in a record.

708

709

710

711

712

713

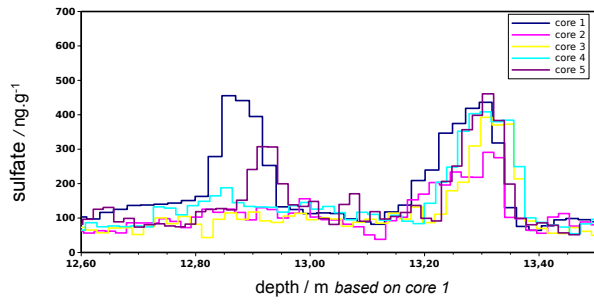
714

715

716

717

718
719
720
721
722
723
724
725



726
727 **Figure 8:** Close look at UE 1809 and Tambora (1815) events showing the absence of the
728 Tambora event in 2 out of the 5 cores. This figure illustrates the possibility of missing major
729 volcanic eruptions when a single core is used.

730

GAUTIER Elsa 16/12/y 16:00
Mis en forme: Interligne : double

731 SOM

732

733 1. Gfeller et al. (2014) method relies on calculating inter-series correlation (expressed as $R_{n,N}$, n being
734 a subset of N time series). To calculate the representativeness of the mean of a given subset of cores,
735 and by letting N going to infinity (simulating a fictive infinite number of cores), Gfeller et al. (2014)
736 use the $\check{R}_{n,\infty}^2$ proxy. We used the same proxy of sulfate representativeness on Dome C 5 cores and
737 obtained the following results:

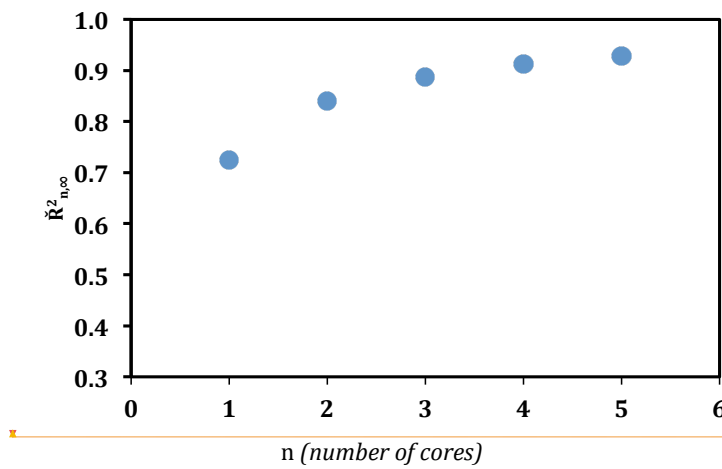
738

n (number of cores)	1	2	3	4	5
$\check{R}_{n,\infty}^2$ SO ₄ ²⁻	0.72	0.84	0.89	0.91	0.93

739

740

741



742

743

744

745 Figure S1: Representativeness of sulfate in the cores ($\check{R}_{n,\infty}^2$) as a function on the number of cores n
746 (based on Gfeller et al., 2014 approach).

747

GAUTIER Elsa 16/12/y 16:00

Mis en forme: Police :11 pt

GAUTIER Elsa 16/12/y 16:00

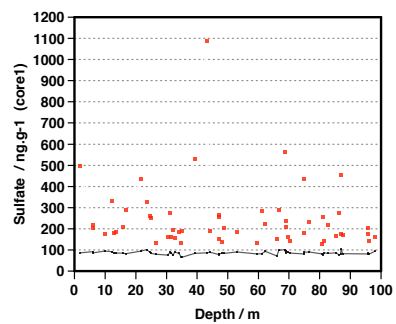
Mis en forme: Police :11 pt

GAUTIER Elsa 14/12/y 21:48

Supprimé: <sp>

Unknown

Mis en forme: Police :14 pt, Gras



749

750 | Figure S2 - Variation of the background along depth in core 1, red dots are detected peaks, the dark
751 | line stands for the background concentration.

752

753